Electronic supplementary information

Reducing non-radiative recombination energy loss via a fluorescence intensifier for efficient and stable ternary organic solar cells

Xuan Liu[a], Yang Liu[a], Yongfeng Ni[ab], Ping Fu[a], Xuchao Wang[a], Qing Yang[ac], Xin Guo[a]* and Can Li[a]*

[a] State Key Laboratory of Catalysis, Dalian Institute of Chemical Physics, Chinese Academy of Sciences; Dalian National Laboratory for Clean Energy, Dalian 116023, P. R. China
[b] Department of Chemical Physics, University of Science and Technology of China, Hefei 230026, P. R. China
[c] University of Chinese Academy of Sciences, Beijing 100049, China
*Corresponding authors, E-mail: guoxin@dicp.ac.cn; canli@dicp.ac.cn

Experimental Section

Materials and methods

The donor polymers PM6, PBDB-T and acceptor small molecules ITIC, IT-4F, and Y6 were purchased from Solarmer Materials Inc. Other intermediate materials were purchased from Adamas, Aldrich, and Alfa and used without any further purification.

Density functional theory (DFT) calculations were carried out at the B3LYP/6-31G(d,p) level using Gaussian 09 program suite. UV-Vis absorption spectra were recorded on a Cary 5000 UV-VIS-NIR spectrophotometer. The photoluminescence spectra were recorded by the fluorescence spectrometer (QM400, PTI). Pure films for PL measurements were controlled at about 60 nm in thickness, and blending films were controlled at about 100 nm. The PLQY values were obtained using an integrating sphere. The photoluminescence excitation wavelength of IT-MCA and IT-4F was 470 nm and 760 nm, respectively, and IT-MCA-containing blend films were

excited at 470 nm. Cyclic voltammetry (CV) was carried out on a CHI600D electrochemical workstation at a scan rate of 50 mV s^{-1} with an Ag/AgCl as the reference electrode. The tapping-mode AFM images were obtained by using a scanning probe microscope on a Bruker Metrology Nanoscope Ⅲ-D. The X-ray diffraction (XRD) tests were carried out on device Rigaku D/Max 2500/PC. ^{1}H-NMR and ^{13}C-NMR spectra were measured on a Bruker 400 MHz AVANCE III with tetramethylsilane as an internal reference. The mass spectroscopy (MS) were measured on an AB SCIEX MALDI-TOF/TOF 5800. The electroluminescence spectrum measurement was conducted by Keithley 2400 SourceMeter by providing bias voltage for the test device. The EQE$_{EL}$ was recorded with an in-house-built system comprising a standard silicon photodiode 1010B, a Keithley 2400 SourceMeter to provide voltage and record injected current, and the emitted light intensity was obtained on a Keithley PR650 spectrometer. The two dimensional Grazing-incidence X-ray diffraction (2D GIXD) patterns were obtained using the beamline BL14B1 at the Shanghai Synchrotron Radiation Facility (SSRF) with the incident photon energy of 10 k eV (wavelength of 1.2398 angstrom) at an incident angle of 0.13° and an exposure time of 60 s. The samples for the 2D GIXD measurement were prepared by spin-coating solutions on Si substrates.

Fabrication and characterization of OPV devices

The photovoltaic devices were fabricated with a structure of glass/ITO/ZnO/active layer/MoO$_3$/Ag. The ITO-coated glass substrates were cleaned by deionized water, acetone, and isopropyl alcohol under ultrasonication for 30 min each and followed by

a UV-ozone treatment for 20 min. Then, ZnO layer was spin-coated (ca. 30 nm thick) onto the cleaned ITO surface. The substrates were then placed into an argon-filled glove box after being baked at 200 °C for 60 min. Subsequently, the active layer of PM6:IT-4F and PBDB-T:ITIC was spin-coated from a 10 mg mL^{-1} (donor:acceptor=1:1, w/w) solution in chlorobenzene (0.5% DIO) at 3000 rpm for 1 min. The PM6:Y6 (1:1.2, w/w) was spin-coated from a 7 mg mL^{-1} solution in chloroform (0.5% CN) at 3000 rpm for 30 s. Finally, 7.5 nm MoO$_3$ and 85 nm Ag layer was deposited on the active layer. The J-V measurement was performed via the solar simulator (SS-F5-3A, Enlitech) along with AM 1.5G spectra whose intensity was calibrated by the certified standard silicon solar cell (SRC-2020, Enlitech) at 100 mV cm^{-2}. The external quantum efficiency (EQE) data were obtained by using the solar-cell spectral-response measurement system (QE-R, Enlitech).

Synthesis of IT-MCA
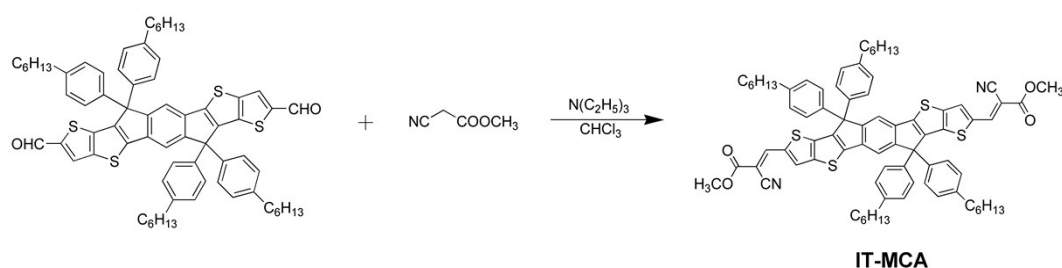
Scheme S1. Synthetic route of IT-MCA.

To a three-necked flask were added IT-CHO (100 mg, 0.1 mmol), methyl cyanoacetate (99 mg, 1 mmol), chloroform (20 mL), and pyridine (0.5 mL). The mixture was refluxed for 20 h under nitrogen atmosphere. After cooling down to room temperature, the reaction mixture was extracted with CH$_2$Cl$_2$ (100 mL), then washed with water (50 mL), dried over Na$_2$SO$_4$. The solvent was removed under reduced

pressure and the residue was purified by column chromatography on silica gel using CH$_2$Cl$_2$ as eluent, yielding a dark green solid (58 mg, 52%). ^{1}H NMR (400 MHz, CDCl$_3$): δ 8.24 (s, 2H), 8.05 (s, 2H), 7.59 (s, 2H), 7.14 (d, 8H), 7.12 (d, 8H), 3.90 (s, 6H), 2.56 (t, 8H) 1.59 (m, 8H), 1.30 (m, 24H) 0.85 (t, 12H). ^{13}C NMR (101 MHz, CDCl$_3$): δ 163.68, 154.72, 150.08, 146.68, 141.11, 138.96, 137.09, 136.33, 128.81, 127.52, 125.81, 99.77, 96.52, 63.22, 53.25, 35.25, 31.45, 31.07, 28.97, 22.42, 14.21. HR-MS (MALDI-TOF): m/z calcd. for (C$_{78}$H$_{80}$N$_2$O$_4$S$_4$) 1236.50 (M+1). Found: 1236.57.
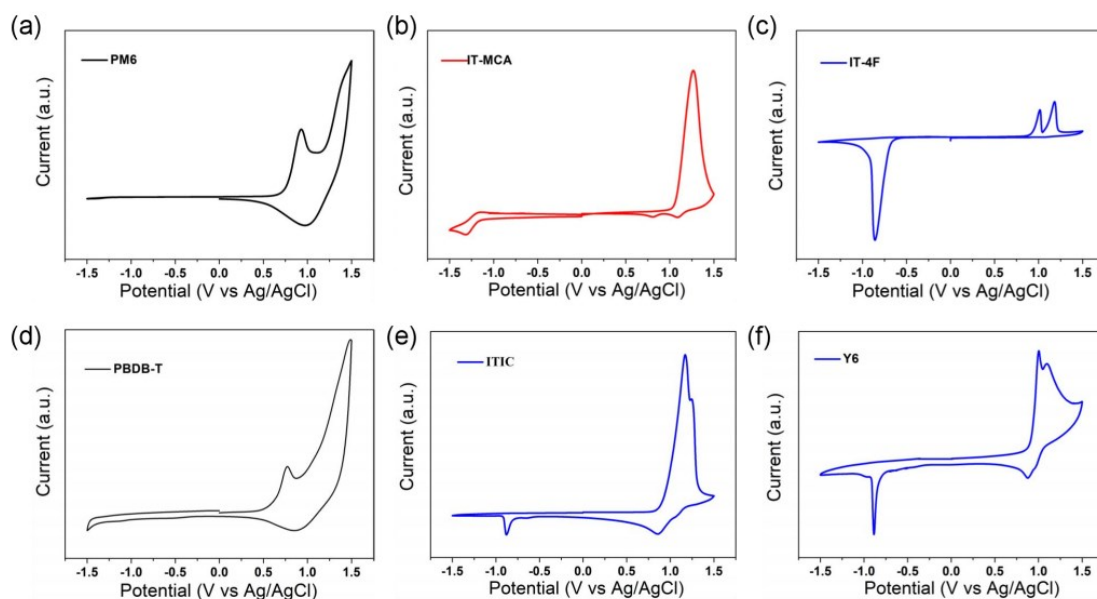
Fig. S1 CV curves of PM6 (a), IT-MCA (b), IT-4F (c), PBDB-T (d), ITIC (e), Y6 (f).
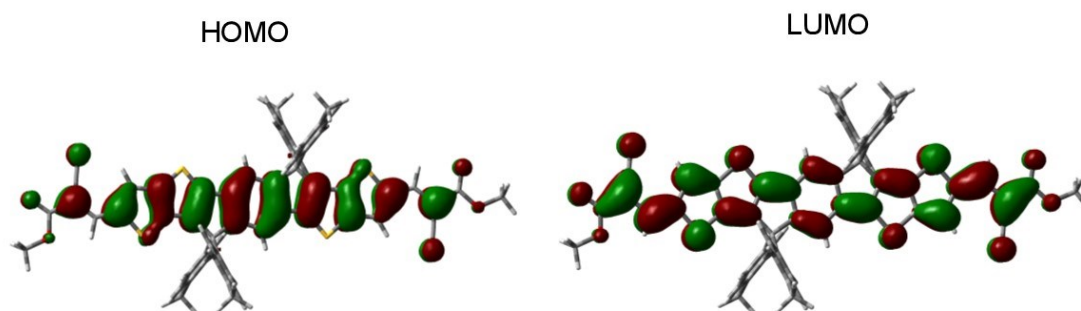
Fig. S2 Optimized electronic density distributions of HOMO and LUMO for the IT-MCA, calculated via Gaussian at the B3LYP/6-31G(d,p) level.
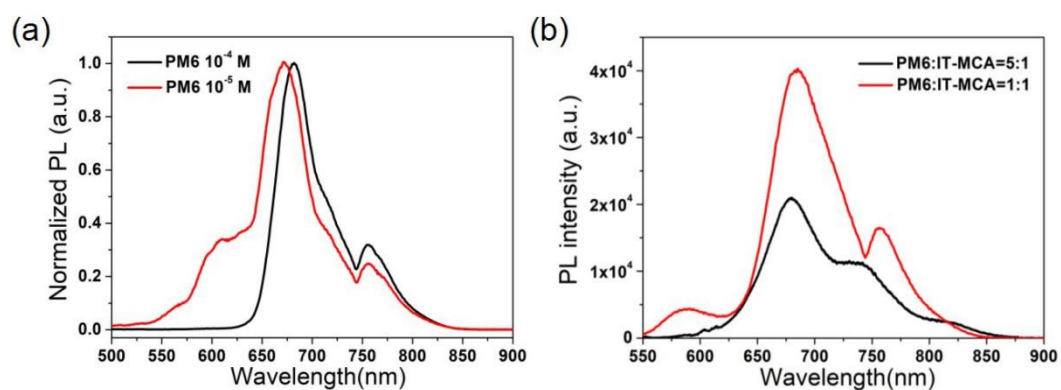
Fig. S3 Steady-state PL spectra of (a) PM6 in solutions and (b) PM6:IT-MCA blend films with different weight ratios.
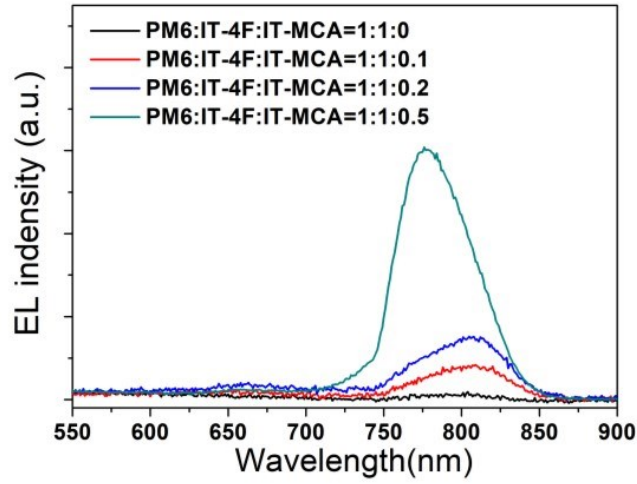
Fig. S4 EL spectra of ternary blend films based on PM6:IT-4F with different IT-MCA ratios.
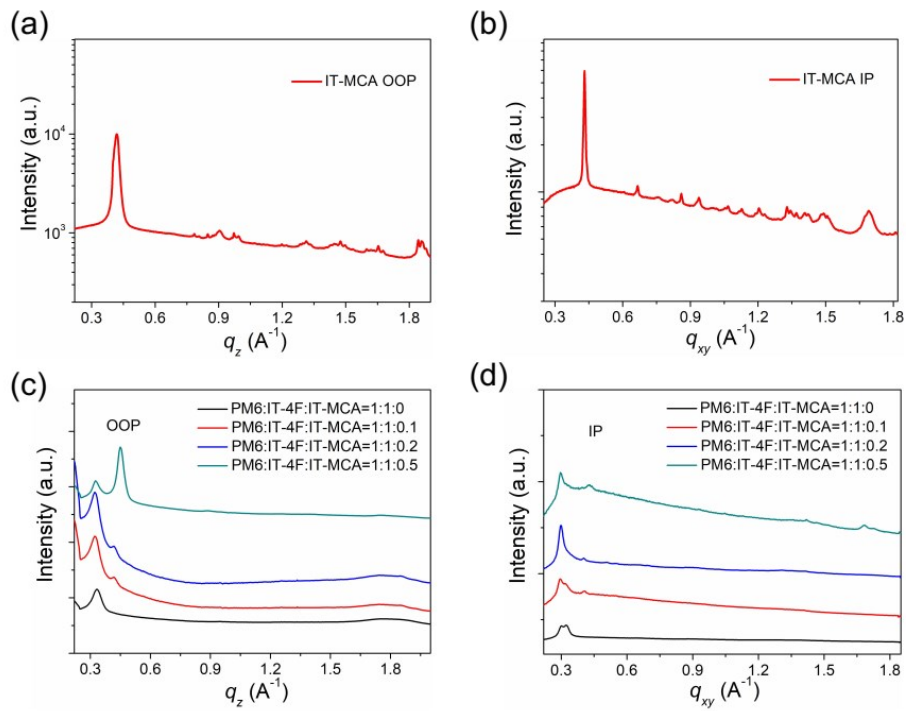
Fig. S5 Out-of-plane (OOP) (a), (c) and In-plane (IP) (b), (d) line cuts for IT-MCA, binary and ternary blend films based on PM6:IT-4F systems with different amounts of IT-MCA.
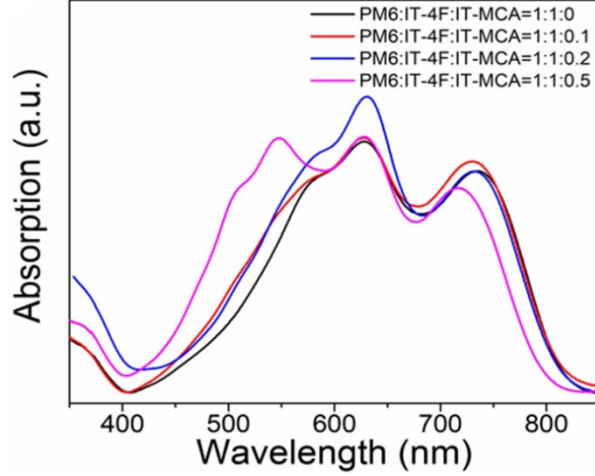
Fig. S6 Absorption spectra of binary and ternary blend films with different IT-MCA ratios.
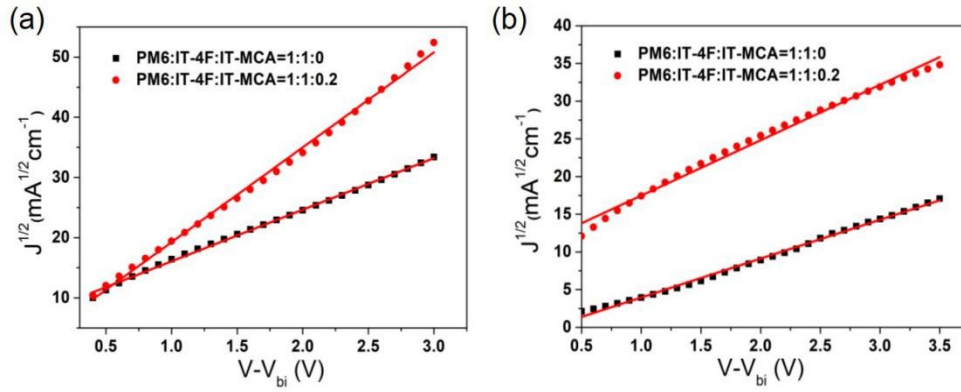
Fig. S7 $J^{1/2}$-V fitting results of the hole-only (a) and electron-only (b) devices based on PBDB-T:acceptor blend films measured by the SCLC method.

The device structures for measurements of the hole and electron mobilities were ITO/PEDOT:PSS/Active layer/MoO$_3$/Au and ITO/ZnO/Active layer/PFN/Al, respectively.

The J–V results were fitted using the Mott–Gurney law that includes field-dependent mobility, given by

$$J = \frac{9}{8}\varepsilon_0\varepsilon_r\mu_0\frac{(V-V_{bi})^2}{d^3}\exp(\beta\sqrt{\frac{V-V_{bi}}{d}})$$

where $\varepsilon_0\varepsilon_r$ is the dielectric permittivity of the active layer, d is the thickness of the active layer, μ_0 the zero-field mobility, and β the field activation factor.
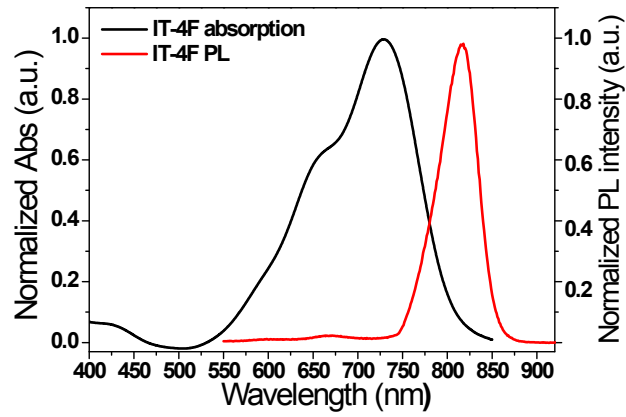
Fig. S8 UV-vis absorption and PL spectra of IT-4F film used to test the E_g.
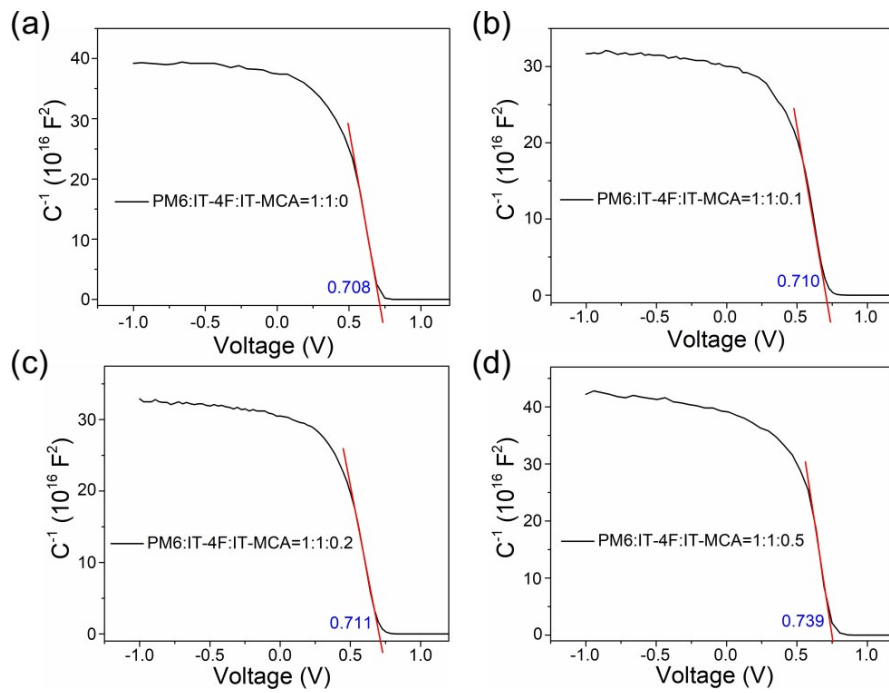
Fig. S9 Mott-Schottky characteristics of the binary and ternary devices measured at 10 kHz in dark.
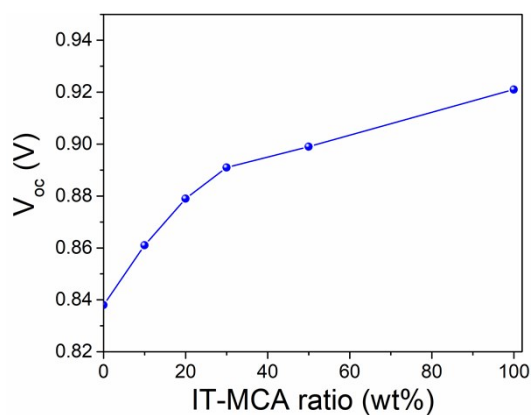
Fig. S10 V_{oc} as a function of weight ratio of IT-MCA.
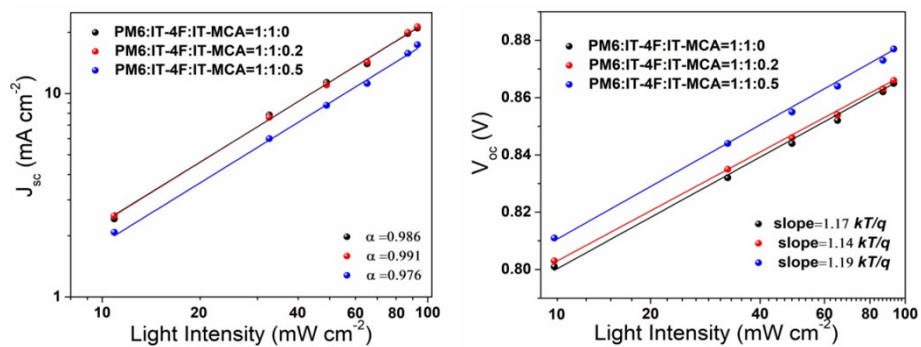
Fig. S11 (a) J_{sc} and (b) V_{oc} as a function of light intensity for the binary and ternary OSCs.
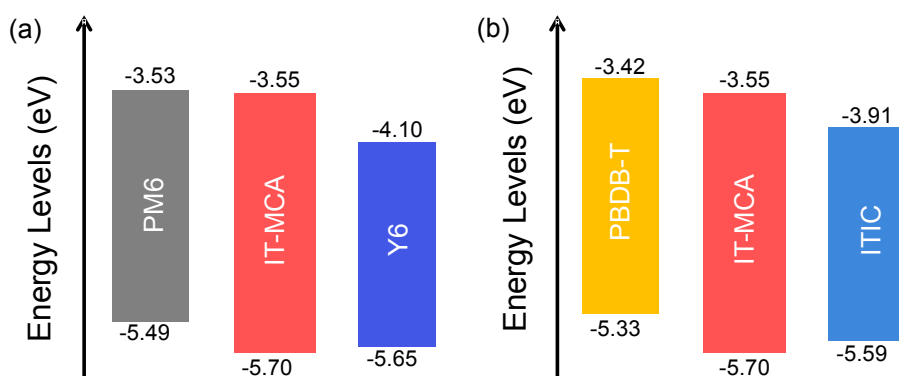
Fig. S12 Energy level diagrams of PM6:Y6 system (a) and PBDB-T:ITIC system (b).
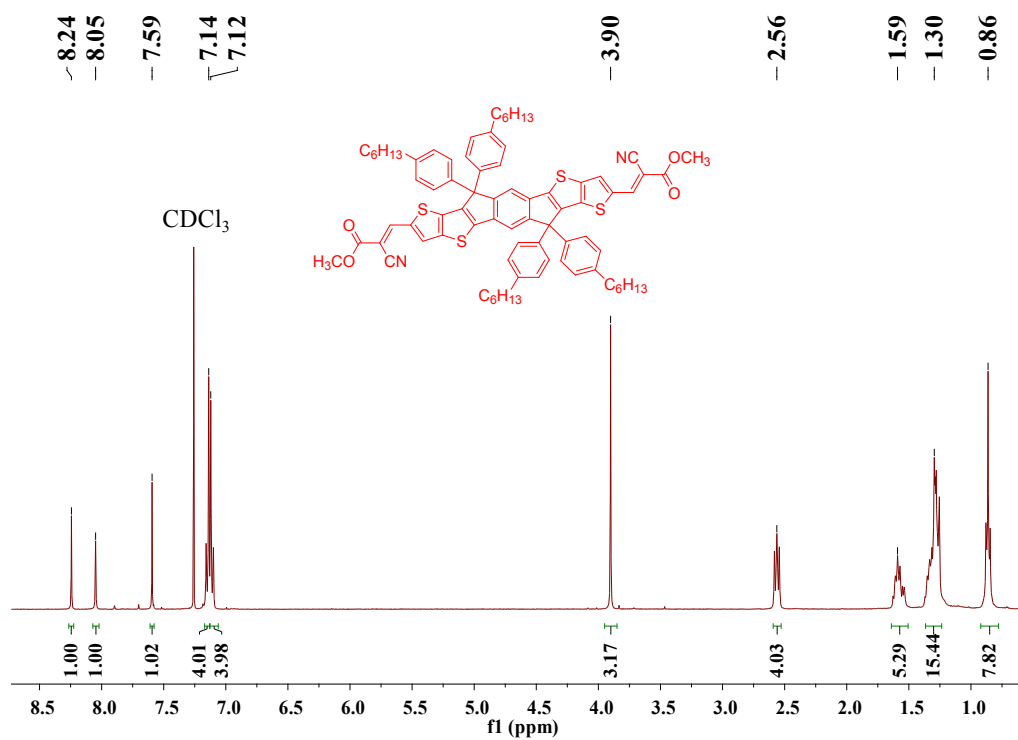
Fig. S13 ¹H NMR spectrum of IT-MCA.
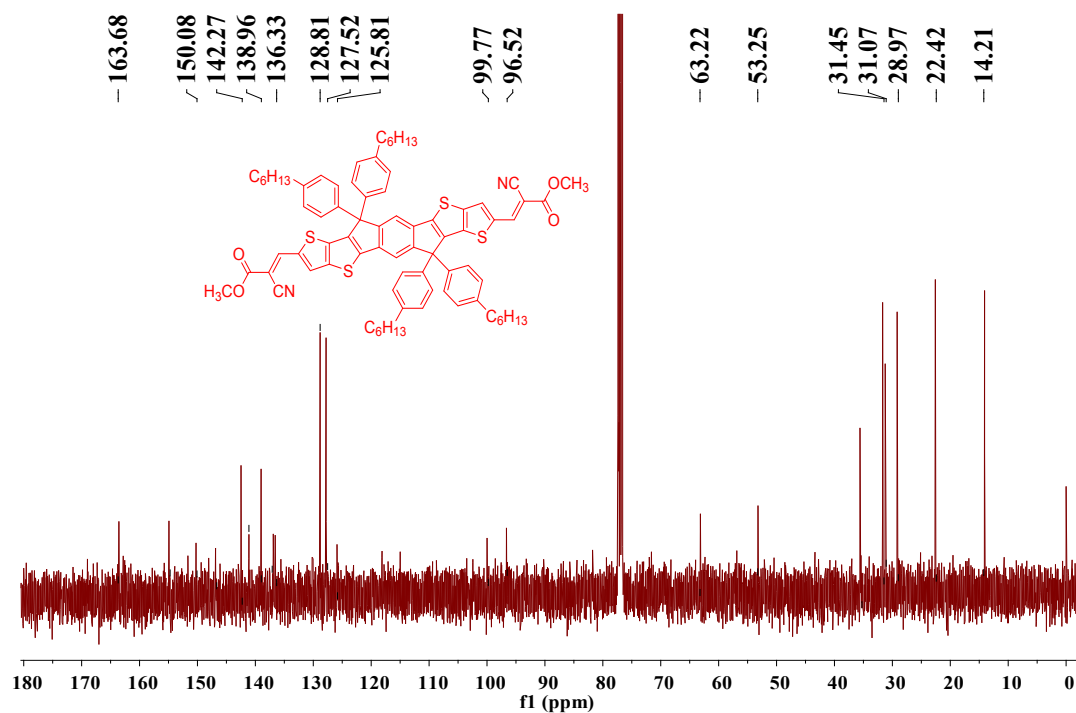
Fig. S14 ¹³C NMR spectrum of IT-MCA.

Table S1. Device performance parameters of binary and ternary OSCs based IT-MCA

Active layer	V_{oc} (V)	J_{sc} (mA cm^{-2})	FF	PCE (%)
PM6:IT-4F:IT-MCA =1:1:0	0.838	19.79	0.74	12.3
PM6:IT-4F:IT-MCA =1:1:0.1	0.861	20.29	0.76	13.2
PM6:IT-4F:IT-MCA =1:1:0.2	0.879	20.98	0.76	14.0
PM6:IT-4F:IT-MCA =1:1:0.3	0.891	18.73	0.71	11.8
PM6:IT-4F:IT-MCA =1:1:0.5	0.899	16.89	0.62	9.4
PM6:IT-4F:IT-MCA =1:1:1	0.921	14.31	0.45	6.0
PM6:IT-4F:IT-MCA =1:0:1	1.220	0.63	0.29	0.2
PM6:IT-4F:IT-MCA =0:1:1	0.291	0.09	0.42	0.01

Table S2. Hole and electron mobilities of binary and ternary blend films.

Samples	Hole mobility (cm^2 V^{-1} s^{-1})	Electron mobility (cm^2 V^{-1} s^{-1})	μ_h/μ_e
PM6:IT-4F:IT-MCA=1:1:0	3.59×10^{-4}	2.16×10^{-4}	1.65
PM6:IT-4F:IT-MCA=1:1:0.2	5.03×10^{-4}	3.28×10^{-4}	1.53

Table S3. Optical and electrical properties of donor, acceptors and IT-MCA.

	$\lambda_{max}^{abs, film}$ (nm)	E_g^{opt} (eV)	HOMO (eV)	LUMO (eV)	E_g^{CV} (eV)
PM6	621	1.85	-5.49	-3.53	1.96
PBDB-T	632	1.80	-5.33	-3.42	1.91
IT-4F	729	1.52	-5.69	-4.10	1.59
Y6	834	1.34	-5.65	-4.10	1.55
ITIC	709	1.57	-5.59	-3.91	1.68
IT-MCA	549	2.10	-5.70	-3.55	2.15